Magnetic Precursor of the Pressure-Induced Superconductivity in Fe-Ladder Compounds

Songxue Chi, Yoshiya Uwatoko, Huibo Cao, Yasuyuki Hirata, Kazuki Hashizume, Takuya Aoyama, and Kenya Ohgushi

The magnetic precursor of the pressure-induced superconductivity in Fe-ladder compound

Songxue Chi,[1] Yoshiya Uwatoko,[2] Huibo Cao,[1] Yasuyuki Hirata,[3]
Kazuki Hashizume,[4] Takuya Aoyama,[4] and Kenya Ohgushi[4,3]

[1] *Quantum Condensed Matter Division, Oak Ridge National Laboratory, Oak Ridge, Tennessee 37831, USA*
[2] *Institute for Solid State Physics (ISSP), University of Tokyo, Kashiwa, Chiba 277-8581, Japan*
[3] *Institute for Solid State Physics, The University of Tokyo,*
Kashiwanoha 5-1-5, Kashiwa, Chiba 277-8581, Japan
[4] *Department of Physics, Graduate School of Science, Tohoku University,*
6-3, Aramaki Aza-Aoba, Aoba-ku, Sendai, Miyagi 980-8578, Japan

The pressure effects on the antiferromagentic orders in iron-based ladder compounds $CsFe_2Se_3$ and $BaFe_2S_3$ have been studied using neutron diffraction. With identical crystal structure and similar magnetic structures, the two compounds exhibit highly contrasting magnetic behaviors under moderate external pressures. In $CsFe_2Se_3$ the ladders are brought much closer to each other by pressure, but the stripe-type magnetic order shows no observable change. In contrast, the stripe order in $BaFe_2S_3$, undergoes a quantum phase transition where an abrupt increase of Néel temperature by more than 50% occurs at about 1 GPa, accompanied by a jump in the ordered moment. With its spin structure unchanged, $BaFe_2S_3$ enters an enhanced magnetic phase that bears the characteristics of an orbital selective Mott phase, which is the true neighbor of superconductivity emerging at higher pressures.

The antiferromagnetic (AF) phase adjacent to superconductivity (SC) is so richly faceted that its microscopic origin still eludes a unified description. Significant variation of the ordered magnetic moment and the underlying degree of electron correlations lie at the heart of the heated dispute [1–3]. The static AF phase in the parent compounds has roughly two categories: stripe magnetism and block magnetism. The former includes the single stripe in LaFeAsO, $BaFe_2As_2$, NaFeAs, and double stripe in FeTe [4]. Spin block order was found in the vacancy-ordered $K_2Fe_4Se_5$ (245) [5]. These materials all have a plane of Fe square lattice once deemed indispensable for the occurence of SC. The recent successful induction of SC by pressure in the ladder compound $BaFe_2S_3$ [6, 7] has introduced a quasi-one dimensional structural motif for the studies of iron-based superconductors and a parallel to the quasi-1D cuprates [8]. As if the layers of the superconducting Fe square lattice were sliced up and staggered, the AFe_2X_3 (A = K, Rb, Cs or Ba and X = Chalcogens) compounds consist of ladders of two-leg Fe-chains with edge-sharing tetrahedra of anions (Se or S) surrounding each Fe site, as shown in Figure 1(a). The reduced dimensionality leads to modified bandwidth [9], Fermi surface topology, and provides a rare insight into critical open issues such as the nature of the AF order.

Both stripe- and block-types of AF orders are hosted by the Fe-ladder compounds. $BaFe_2S_3$ and $CsFe_2Se_3$, with the $CsCu_2Cl_3$ type structure ($Cmcm$ space group), have the stripe AF order where the ferromagnetic (FM) spin pairs on the same ladder rung correlate antiferromagnetically along the leg direction. The ordered moment lies in the rung-direction in $BaFe_2S_3$ (Fig.1(b))[6]

and the leg-direction in $CsFe_2Se_3$ (Fig.1(c)) [10]. In $BaFe_2Se_3$, the distorted $FeSe_4$ tetrahedron lose the C-centering and result in the lowered symmetry $Pnma$ [11]. The magnetic structure consists of blocks of 4 FM spins forming alternating AF pattern along the leg direction [12]. The magnetic excitations in $BaFe_2Se_3$ fits the description of localized spins and an orbital-selective Mott phase [13].

The pressure-induced metal-insulator transition in $BaFe_2S_3$ is categorized as a bandwidth-control type Mott transition [6, 7]. The AF order is suppressed before SC arises at higher pressures [7]. To elucidate the SC pairing mechanism, the detailed evolution of the AF phase under pressure is the crucial step still missing. In this Letter, we present a pressure effect study on the AF orders in the single crystalline $CsFe_2Se_3$ and $BaFe_2S_3$ using neutron diffraction. The two compounds contrast in ladder
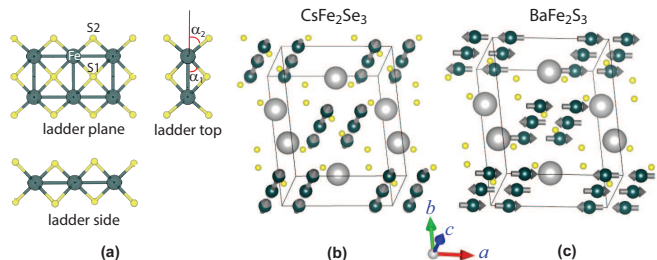

FIG. 1: (color online) (a) The structure of the Fe-ladder and its relative positions with anions (Se or S) for the ladder compounds adopting the $Cmcm$ space group. The magnetic structure in (b) $CsFe_2Se_3$ with spins parallel to the c-axis and (c) in $BaFe_2S_3$ with ordered moment along a.

spacings and electronic properties. We show that they also exhibit highly contrasting responses to pressures. The magnetism in $CsFe_2Se_3$ is robust against the applied pressures close to 2 GPa. The AF order in $BaFe_2S_3$ undergoes a rather abrupt enhancement around 1 GPa, both in transition temperature and ordered moment, before being suppressed at higher pressures. Such unusual change qualifies as an orbital selective Mott transition.

Single crystals of $BaFe_2S_3$ and $CsFe_2Se_3$ were prepared by the solid-state reaction method [6]. The samples were inserted into Teflon capsules and loaded in a piston cylinder cell made of CuBe alloy or Zr-based metallic glass [14]. Daphne oil was used as the pressure transmitting medium. The single crystal neutron diffraction measurements were carried out on HB-3A Four-circle Diffractometer at the High Flux Isotope Reactor (HFIR) of the Oak Ridge National Laboratory (ORNL). The wavelengths of 1.003 Å and 1.542 Å were employed. The pressures were calibrated with NaCl single crystal loaded together with the sample in the cell [16]. One of the applied pressures was calibrated on the Wide Angle Neutron Diffractometer (WAND) at HFIR. The Rietveld refinements on the crystal and magnetic structures were conducted using the FullProf Suite [15].

We report the structural information at 4 K. Both compounds can be well-described by the orthorhombic space group $Cmcm$. The lattice constants of $CsFe_2Se_3$ are a=9.7105(9) Å, b=11.595(1) Å, and c=5.6659(3) Å. The lattice constants and structrual parameters of $BaFe_2S_3$ are summarized in Table I. The biggest contrast is in a, which means the ladders in the same row are closer in $BaFe_2S_3$ since the two compounds have almost the same rung length. The ladder leg is bigger in $CsFe_2Se_3$. Moderate hydraulic pressure changes the spacings between the ladders and does little to the size of the ladders.

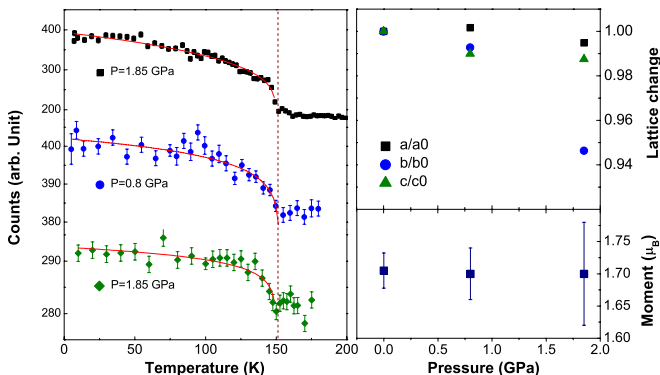At ambient pressure, the magnetic reflections for both

TABLE I: Structural parameters for $BaFe_2S_3$ at 4 K at ambient pressure (top) and 1.3 GPa (bottom). The ambient pressure lattice constants are a=8.8607(4) Å, b=11.2767(6) Å, and c=5.2730(6) Å. The length of the ladder rung is 2.727 Å and that between rungs is $c/2$=2.6365 Å. Those for 1.3 GPa are a=8.6172(4) Å, b=11.0169(1) Å, and c=5.2159(5) Å. The length of the ladder rung is 2.701 Å and that between rungs is $c/2$=2.608 Å.

Atom	site	x	y	z
Ba	$4c$	1/2	0.181(4)	1/4
Fe	$8e$	0.3461(8)	1/2	0
S(1)	$4c$	1/2	0.612(9)	1/4
S(2)	$8g$	0.2091(2)	0.364(5)	1/4
Ba	$4c$	1/2	0.185(3)	1/4
Fe	$8e$	0.343(2)	1/2	0
S(1)	$4c$	1/2	0.613(7)	1/4
S(2)	$8g$	0.210(7)	0.374(5)	1/4

compounds were collected using the propagation wave vector (1/2,1/2,0). Representation analysis provides four different irreducible representations (irreps) Γ_1, Γ_2, Γ_3 and Γ_4, each of which consists of 3 basis vectors (BV)[16]. We sort through all BVs in each irrep for refinement and obtained the best R-factor from ϕ_9 for $CsFe_2Se_3$ and ϕ_1 for $BaFe_2S_3$. The ordered moment of 1.705(27) μ_B lies along the c-direction in $CsFe_2Se_3$ [Fig. 1(c)]. The magnetic peak intensity as a function of temperature was fitted to a power law, plotted as the red curves in Fig. 2(a), which gives the Néel temperature, T_N. T_N is estimated to be 149 K. These findings are all consistent with the previous powder diffraction study [10]. The refined moment in $BaFe_2S_3$ is 1.043(30) μ_B along the a-direction, as shown in Fig. 1(c), which is smaller than the reported 1.20(6) μ_B in ref.[6]. Its AF transition temperature, T_N=105 K [Fig. 3(a)], is also lower than the reported 119 K in Ref.[6]. The slightly weaker AF order in the present sample can be explained by the strong dependence of magnetic properties on the synthetic procedure [6].

For both compounds, identical crystals were pressurized for the pressure measurements. We first discuss the effect of pressure on $CsFe_2Se_3$, as summarized in Fig. 2. The magnetic wave vector remains unchanged up to the highest applied pressure (1.85 GPa). The magnetic intensity at (0.5,2.5,1) develops about the same temperature at 0.9 GPa (152 K) and 1.85 GPa (150 K) as the ambient pressure (149 K). Rietveld fits confirmed the unchanged nuclear structure and spin configuration under the two pressures. The size of the ordered moment also remains the same [Fig. 2(c)]. The lattice constants decrease at different rates under pressure. At 1.85 GPa, a and c decrease by less than 2%, but b decreases by more than 5% and becomes 11.22 Å. The distance between the ladder stacking layers in $CsFe_2Se_3$ under 2 GPa is even slightly

FIG. 2: (color online) The effect of pressure on structural and magnetic properties in $CsFe_2Se_3$. (a) The temperature dependence of the (0.5,2.5,1) peak intensity at ambient pressure, 0.8 GPa and 1.85 GPa. (b) The change of lattice constants under various pressures. (c) The size of the ordered moment at different pressures.
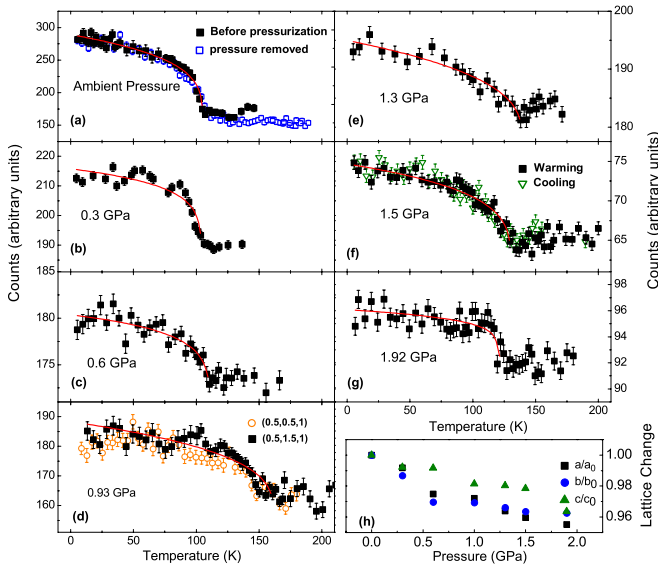
FIG. 3: (color online) The temperature variation of the magnetic peak intensities in BaFe$_2$S$_3$ at different pressures. (a) (0.5,1.5,1) at the ambient pressure before the hydraulic pressure is applied and after the pressure has been removed (b) (0.5,2.5,1) at the pressure of 0.3 GPa (c) (0.5 1.5,1) at 0.6 GPa (d) (0.5,0.5,1) (orange open circle) and (0.5,1.5,1) (black solid square) at 0.93 GPa. The power law fit is for (0.5,1.5,1) (e) (0.5,1.5,1) at 1.3 GPa (f) (0.5,1.5,1) on warming and cooling at 1.5 GPa and (g) (0.5,1.5,1) at 1.93 GPa. (h) The change of lattice parameters as a function of pressure.

FIG. 4: (color online) Pressure-temperature phase diagram of BaFe$_2$S$_3$ showing the AF and superconducting transitions. Black solid circles correspond with the result of present study while other symbols represent the results from Ref. [6]. The inset shows the size of ordered moment of the stripe magnetic phase as a function of pressure.

smaller than that in unpressurized BaFe$_2$S$_3$.

In contrast to the strong magnetic order in CsFe$_2$Se$_3$, the magnetic phase in BaFe$_2$S$_3$ exhibits remarkable sensitivity to pressures. Fig. 3(b) shows the order parameter at the pressure of 0.3 GPa. T_N is estimated to be 104 K, which implies that the AF order is unaffected. At 0.6 GPa, (0.5,0.5,0) remains as the magnetic propagation wavevector. T_N shows a slight increase to 112 K [Fig.3(c)]. The Rietveld refinements using intensities of rocking curve scans collected at 0.6 GPa show no major change of crystal and spin structures. The variation of refined moment, 1.02(8) μ_B, from the ambient pressure value is smaller than the statistical error.

As pressure is increased to 0.95 GPa, a drastic change of the magnetic order occurs. The change of (0.5,1.5,1) intensity on warming shows that the magnetic transition becomes 164 K, a leap of 56% from the ambient pressure and 47% from 0.6 GPa [Fig. 3(d)]. The increase of T_N at such a rapid rate, 132.5 K/GPa, is unprecedented. To confirm this dramatic effect of pressure we perform the same temperature measurement on another magnetic reflection (0.5,0.5,1), as represented by the orange open circle in Fig. 3(d), which shows the same T_N. To obtain the correct spin structure of the pressure-strengthened magnetic phase, we made broad surveys on the potential magnetic reflection positions. Using the area detector and varied temperature we ruled out the possibility of a
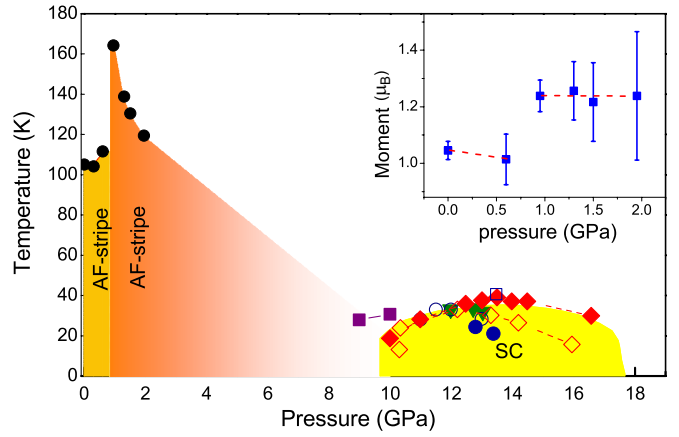
different magnetic wave vector [16]. All the real magnetic peaks were found at the $(m/2, n/2, l = 1)$ (m and n are intergers) positions. The Fullprof refinement using these peaks yielded the best R factor with the same ϕ_1 of Γ_1, an unchanged structure, and revealed that the ordered moment jumped to 1.24(5) μ_B.

Further increase of pressure immediately starts to suppress T_N. It decreases to 139 K at 1.3 GPa [Fig. 3(e)] and to 131 K at 1.5 GPa [Fig. 3(f)]. The order parameter on cooling shows no hysteresis, suggesting the glassy behavior in Ba$_{1-x}$Cs$_x$Fe$_2$Se$_3$ [17] and Ba$_{1-x}$K$_x$Fe$_2$S$_3$ [18] is likely caused by the change of carrier concentrations. Fig. 3(g) shows a continued suppression of T_N to 119 K at 1.93 GPa. We carried out refinements for all pressures above 0.95 GPa, which show that the same stripe type of magnetic order and the same value of moment persists to the highest measured pressure. After depressurization, the order parameter measurement was taken on the same sample which shows the original value of T_N, as shown by the open blue square in Fig. 3(a).

To obtain more information on the crystal structure at pressures above the sharp change in AF order, we used a pressure cylinder made of Zr-based metallic glass for $P = 1.3$ GPa. The material does not produce sharp Bragg reflections [14] and allowed us to collect more Bragg reflections from the sample. The refined structural parameters at 1.3 GPa, together with those at ambient pressure, are summarized in Table I.

Our neutron results of the magnetic evolution in BaFe$_2$S$_3$ under hydraulic pressure are summarized in the $P - T$ phase diagram in Fig. 4, along with the pressure-induced SC phase from Ref.[6]. The refined moment sizes at various pressures are shown in the inset of Fig. 4. For pressures higher than 2 GPa, we know the sup-

pression of the magnetic order continues untill the SC starts[7]. We separate the AF phases below and above 0.95 GPa with two colors, the boundary of which represents a pressure-induced magnetic phase transition manifested by a tremendously boosted T_N, accompanied by a jump in the ordered moment. SC occurs in this $Cmcm$ ladder structure [6], thus this pressure-enhanced stripe-type AF order is the true of precursor of the spin fluctuations that might correspond with the SC state.

The absence of structural transitions under pressure in these two ladder compounds is to be expected because the $Cmcm$ phase is very stable. Both pressure and heating can drive a $Pnma$ to $Cmcm$ structural transition in $BaFe_2Se_3$ [19]. Such a transition can also be achieved by chemical pressure as in $Ba_{1-x}Cs_xFe_2Se_3$ [17]. The $Cmcm$ phase has two nonequivalent anion sites, in case of $BaFe_2S_3$, S1 and S2. As shown in Fig. 1(a), S1 is between the ladder legs and S2 is out of the ladder. Not only do the two S sites have different distances from Fe, but also different heights above the ladder plane. This makes the point symmetry surrounding the Fe ions C_s instead of S_4 as in the 2D Fe compounds. Such deviation implies different crystal field schemes and orbital states in the $Cmcm$ ladder compounds. The differences between the two S sites are further increased by pressure in $BaFe_2S_3$. Compared to ambient pressure, the Fe-S1 distance at 1.3 GPa decreases from 2.285 to 2.258 Å and Fe-S2 decreases from 2.269 to 2.237 Å. The angles α_1 and α_2, as defined in Fig. 1(a), changes from 43.65° to 42.90° and from 48.55° to 49.55°, respectively. The change in the size the Fe ladder is smaller than the standard error.

The valence of Fe ions in $CsFe_2Se_3$ is supposed to be a formal mixed +2.5. However Mossbauer [10] and photoemission [20] studies indicate that all the Fe sites take the Fe^{2+} configuration and the Se $4p$ holes are trapped at the Se sites between the two legs [20]. The localized Se $4p$ holes and thus the Fe $3d$ electrons make $CsFe_2Se_3$ a charge-transfer-type Mott insulator, and are essential in stabilizing the stripe-c magnetic phase. Substituting Ba with K in $BaFe_2Se_3$ [9] results in the switch from the block magnetic phase to stripe-c phase. Similarly, doping Cs [17] triggers a switch from block to stripe-a, then to stripe-c. In both cases, the transition to stripe-c order is accompanied by an increase in variable range hopping, indicating the localization of carriers. The dominating transfer integral is between the nearest neighbor $d_{3z^2-r^2}$ orbitals [10, 21], which is along the leg direction. The long Fe-Fe bond distances along the leg direction, u=2.83 Å in $CsFe_2Se_3$, as opposed to u=2.63 Å in $BaFe_2S_3$, also helps to localize the charges and stabilize the stripe-c order. The pressure does not shorten the rung enough to disturb the magnetic order even though the ladders are brought much closer. This indicates that the inter-ladder exchange interaction and transfer integral in the ladder compounds are small.

In comparison, $BaFe_2S_3$ is not an insulator but a semiconductor with a small energy gap of 0.06-0.07 eV [22, 23]. Localized Fe $3d$ electrons coexist with itinerant electrons [20]. In a localized regime, if the exchange interaction is affected by the pressure through the compressed lattices, the pressure dependence of the AF transition temperature follows the Bloch's rule [24]. The smooth variation of lattices would result in a gradual increase of T_N, as in Fe_3O_4 [25] and $La_{1.4}Sr_{1.6}Mn_2O_7$ [26]. This is certainly not the case for $BaFe_2S_3$. In an itinerant picture, on the other hand, the pressure can potentially modify the Fermi pockets [21] to improve the nesting feature, but neither hole- nor electron-doping produces such drastic magnetic enhancement [18, 27]. If the pressure indeed reduces correlation, by increasing the bandwidth and decreasing U [21], and subsequently delocalizes Fe $3d$ electrons, the increased hopping on the ladder rungs, through some double exchange mechanism, should be able to enhance the FM interactions. This would explain the increased T_N, but not the increased moment.

The simultaneous spring of T_N and the ordered moment at about 1 GPa signals a quantum phase transition (QPT) that eludes first principle studies [21, 28, 29]. This QPT ushers the $BaFe_2S_3$ system into the true Mott phase whose gap closes at higher pressures to pave the way for the SC phase [7]. It has the apparent fingerprints of an orbital selective Mott transition (OSMT): (i) The unchanged magnetic structure and spin orientation rule out the possibility of a metamagnetic transition. (ii) The change of moment and its two-stage saturation has been predicted by the theories of OSMT [3, 30–33]. In these theories, change of occupancies of $3d$ orbitals brings half-filled t_{2g} shell that can be readily localized. In our case, the sulfur tetrahedron modified by pressure may increase the crystal field splitting, which in turn changes the orbital occupancies. With a robust Hund's interaction that decouples bands [34], the localization only needs to happen to one of five $3d$ orbitals, all of which contribute to the AF order [28]. (iii) The maximum value of T_N at the pressure-induced QPT is also characteristic of Mott critical coupling under the influence of strong Hund's rule coupling [35, 36]. (iv) An unknown transition at about 200 K [7, 18] tends to decrease and merge with T_N as pressure increases [7, 20]. This transition is possibly related to orbital ordering and hints of the critical role of the orbitals in forming the magnetic ground state in $BaFe_2S_3$.

In summary, moderate hydraulic pressure up to 2 GPa exposes contrasting magnetic stability in two Fe-based ladder compounds with identical crystal structures and similar spin structures. In $CsFe_2Se_3$ the stripe-type magnetic phase with c-direction spins remains unfazed up to the highest measured pressure, while the a-direction stripe order in $BaFe_2S_3$ goes through a QPT at about P=1GPa where both the Néel temperature and the ordered moment abruptly increased. This QPT has the signature of an OSMT. Such a finding in a quasi 1D system

can narrow down the theoretical scope in determining the universal physics that drives the diverse magnetism in iron-based compounds.

[1] Pengcheng Dai, J. P. Hu, and E. Dagotto, Nature Physics **8**, 709 (2012).

[2] Q. Si, R. Yu, and E. Abrahams, Nature Reviews Materials **1**, 16017 (2016).

[3] Z. P. Yin, K. Haule, and G. Kotliar, Nature Materials **10**, 932 (2011).

[4] Pengcheng Dai, Rev. Mod. Phys. **87**, 855 (2015).

[5] W. Bao, Q. Z. Huang, G. F. Chen, and M. A. Green, D. M. Wang, J. B. He, and Y. M. Qiu, Chinese Physics Letters **28**, 086104 (2011).

[6] H. Takahashi, A. Sugimoto, Y. Nambu, T. Yamauchi, Y. Hirata, T. Kawakami, M. Avdeev, K. Matsubayashi, F. Du, C. Kawashima, H. Soeda, S. Nakano, Y. Uwatoko, Y. Ueda, T. J. Sato, and K. Ohgushi, Nature Materials, **14**, 1008 (2015).

[7] T. Yamauchi, Y. Hirata, Y. Ueda, and K. Ohgushi, Physical Review Letters **115**, 246402 (2015).

[8] M. Uehara, T. Nagata, J. Akimitsu, H. Takahashi, N. Mori, K. Kinoshita, Journal of the Physical Society of Japan, **65**,2764 (1996).

[9] J. M. Caron, J. R. Neilson, D. C. Miller, K. Arpino, A. Llobet, and T. M. McQueen, Physical Review B **85**, 180405(R) (2012).

[10] F. Du, K. Ohgushi, Y. Nambu, T. Kawakami, M. Avdeev, Y. Hirata, Y. Watanabe, T. J. Sato, and Y. Ueda, Physical Review B **85**, 214436(R) (2012).

[11] H. Y. Hong, and H. Steinfin, Journal of Solid State Chemistry **5**, 93 (1972).

[12] Y. Nambu, K. Ohgushi, S. Suzuki, F. Du, M. Avdeev, Y. Uwatoko, K. Munakata, H. Fukazawa, S. Chi, Y. Ueda, and T. J. Sato, Physical Review B **85**, 064413 (2012).

[13] M. Mourigal, S. Wu, M. B. Stone, J. R. Neilson, J. M. Caron, T. M. McQueen, and C. L. Broholm, Physical Review Letters **115**, 047401 (2015).

[14] K. Komatsu, K. Munakata, K. Matsubayashi, Y. Uwatoko, Y. Yokoyama, K. Sugiyama, and M. Matsuda, High Pressure Research **35**, 254 (2015).

[15] J. Rodriguezcarvajal, Physica B **192**, 55 (1993).

[16] See Supplemental Material for details.

[17] T. Hawai, Y. Nambu, K. Ohgushi, F. Du, Y. Hirata, M. Avdeev, Y. Uwatoko, Y. Sekine, H. Fukazawa, J. Ma, *et al.*, Physical Review B **91**, 184416 (2015).

[18] Y. Hirata, S. Maki, J. I. Yamaura, T. Yamauchi, and K. Ohgushi, Physical Review B **92**, 205109 (2015).

[19] V. Svitlyk, D. Chernyshov, E. Pomjakushina, A. Krzton-Maziopa, K. Conder, V. Pomjakushin, R. Pottgen, V. Dmitriev, Journal of Physics-Condensed Matter **25**, 315403 (2013).

[20] D. Ootsuki, N. L. Saini, F. Du, Y. Hirata, K. Ohgushi, Y. Ueda, and T. Mizokawa, Physical Review B **91**, 014515 (2015).

[21] R. Arita, H. Ikeda, S. Sakai, and M. T. Suzuki, Physical Review B **92**, 054515 (2015).

[22] W. M. Reiff, I. E. Grey, A. Fan, Z. Eliezer, and H. Steinfink, Journal of Solid State Chemistry **13**, 32 (1975).

[23] Z. S. Gonen, P. Fournier, V. Smolyaninova, R. Greene, F. M. Araujo-Moreira, and B. Eichhorn, Chemistry of Materials **12**, 3331 (2000).

[24] D. Bloch, Journal of Physics and Chemistry of Solids **27**, 881 (1966).

[25] G. A. Samara, and A. A. Giardini, Physical Review **186**, 577 (1969).

[26] K. V. Kamenev, G. J. McIntyre, Z. Arnold, J. Kamarad, M. R. Lees, G. Balakrishnan, E. M. L. Chung, and D. M. Paul, Physical Review Letters **87**, 167203 (2001).

[27] M. Reissner, W. Steiner, and H. Boller, Hyperfine Interactions (C), Vol 5, Proceedings, pp. 197-200 (2002).

[28] M. T. Suzuki, R. Arita, and H. Ikeda, Physical Review B **92**, 085116 (2015).

[29] Q. L. Luo, A. Nicholson, J. Rincon, S. H. Liang, J. Riera, G. Alvarez, L. M. Wang, W. Ku, G. D. Samolyuk, A. Moreo, and E. Dagotto, Physical Review B **87**, 024404 (2013).

[30] L. de' Medici, S. R. Hassan, M. Capone, and X. Dai, Physical Review Letters **102**, 126401 (2009).

[31] P. Werner, and A. J. Millis, Physical Review Letters **99**, 126405 (2007).

[32] P. Werner, E. Gull, M. Troyer and A. J. Millis, Physical Review Letters **101**, 166405 (2008).

[33] J. Rincon, A. Moreo, G. Alvarez, and E. Dagotto, , Physical Review Letters **112**, 106405 (2014).

[34] L. de' Medici, Physical Review B **83**, 205112 (2011).

[35] L. de' Medici, J. Mravlje, and A. Georges, Physical Review Letters **107**, 256401 (2011).

[36] J. Mravlje, M. Aichhorn, and A. Georges, Physical Review Letters **108**, 197202 (2012).